



On the structure and variability of atmospheric circulation regimes in coupled climate models

Antje Weisheimer*, Dörthe Handorf and Klaus Dethloff

Alfred Wegener Institute for Polar and Marine Research, Research Department, Potsdam, Germany

Abstract: In order to investigate whether climate models of different complexity have the potential to simulate natural atmospheric circulation regimes, 1000-year-long integrations with constant external forcing have been analysed. Significant non-Gaussian uni-, bi-, and trimodal probability density functions have been found in 100-year segments.

© 2001 Royal Meteorological Society

Keywords: Unforced climate variability, atmospheric circulation regimes.

1. INTRODUCTION

In the recent debate on climate change and global warming, one of the central problems is the confidence in estimations and distinctions of anthropogenic vs natural variability. Assuming the atmosphere to be almost intransitive (Lorenz, 1968), climate variability will be manifest primarily in terms of changes to the frequency of occurrence of preferred circulation states (Palmer, 1999). Since the geographical response patterns of any external forcing (e.g. anthropogenic) can in principle project onto natural variability modes, understanding the structure of these intrinsic patterns of variability is of fundamental importance.

The dynamical paradigm is supported by Corti *et al.* (1999) on the basis of atmospheric circulation data. During the last ~40 years, when the atmosphere was supposed to be most strongly forced by enhanced global warming, the probability density of the preferred tropospheric circulation modes did alter, although the spatial patterns themselves stayed the same. Corti *et al.* (1999) concluded that the observed tropospheric warming of the northern hemisphere (NH) could not *a priori* be linked to any anthropogenic forcing pattern, but manifested itself in a changing frequency of occurrence of preferred circulation regimes. Since the detection and prediction of climate change are largely based on modelling studies, climate models able to simulate natural circulation regimes and their associated variability correctly, are a necessary prerequisite.

* Corresponding author. Telegrafenberg A43, D-14473 Potsdam, Germany. E-mail: weisheim@awi-potsdam.de

Recently, [Monahan *et al.* \(2000\)](#) determined the optimal nonlinear approximation to data produced by long-term runs of a coupled general circulation model (GCM) by means of a nonlinear principal component analysis. A prescribed enhanced CO₂ forcing results in changes of the occupation statistics and thus is broadly consistent with the above-mentioned perspective.

Here we investigate the characterization and temporal variability of the tropospheric regime behaviour in the NH using 1000-year-long unforced control integrations of two coupled atmosphere-ocean models with different complexity. Following [Corti *et al.* \(1999\)](#) natural hemispheric-scale circulation regimes defined as cluster anomalies corresponding to local density maxima in a low-dimensional phase space will be examined in order to find out whether the different models are able to simulate similar atmospheric modes. Furthermore, the structure and variability of modelled regimes of the atmospheric circulation will be studied.

2. MODEL DESCRIPTION

Control integrations with fixed external forcing parameters over 1000 years of two global coupled atmosphere-ocean models of different complexity have been investigated. The simplified climate model (SCM) resolves explicitly the large-scale structures in the atmosphere and the ocean, whereas a statistical description by second order moments in dependence on the large scale circulation is used for the synoptic components ([Petoukhov *et al.* 1998](#)). The model equations for large scale processes follow by averaging the primitive thermo-hydrodynamic equations and applying a scale analysis. The vertical integration has been performed under the assumption of a universal vertical structure of the climate variables. The atmosphere is divided into eight layers from the surface up to a height of 80 km. The ocean model considers three vertical layers. The horizontal atmospheric grid boxes have a size of $6 \times 4.5^\circ$. The simplifications of the model allow a time step of 5 days. In the model the fundamental physical processes are considered, such as radiative transfer, small and large scale horizontal/vertical transports of momentum, heat and moisture, cloud and precipitation physics, exchange between soil, vegetation and atmosphere. A detailed description of the model's long-term performance is given in [Handorf *et al.* \(1999\)](#).

The second model used, the GCM ECHAM3/LSG, consists of the atmospheric part ECHAM3 ([Roeckner *et al.*, 1992](#)) and the ocean model LSG ([Maier-Reimer *et al.*, 1993](#)). It is based on the full set of the atmospheric primitive equations. Processes as radiation, clouds, precipitation, convection and diffusion have been parameterized. The vertical resolution of the atmosphere is given by 19 layers reaching from the ground up to 10 hPa. The horizontal spectral resolution of T21 corresponds with a Gaussian grid of $5.6 \times 5.6^\circ$. The thermodynamical ocean model includes 11 vertical layers and was run at a $4 \times 4^\circ$ horizontal resolution. Aspects of the interdecadal variability of this control integration have been analysed by e.g. [Timmermann *et al.* \(1998\)](#) and [Perlwitz *et al.* \(2000\)](#).

3. METHOD OF DEFINING CIRCULATION REGIMES

The main NH tropospheric circulation regimes have been determined on the basis of monthly mean winter (DJF) data which characterize the flow of the free atmosphere, i.e. the pressure field at 5.5 km simulated by the SCM and the geopotential height at 500 hPa simulated by the ECHAM3/LSG. The spin up periods are excluded from the analysis. After removing the mean seasonal cycle the data have been projected onto empirical orthogonal functions (EOF). To calculate these EOF patterns, the data have been detrended further by taking deviations from a 5-year running mean. The first two EOF patterns of variability form the orthogonal basis vectors of the reduced phase space.

The dominant spatial mode (EOF 1) of the ECHAM3/LSG model explains 28% of the total variance and resembles the Arctic Oscillation (AO) (Thompson and Wallace, 1998) as a quasi-zonally symmetric annular mode of variability with a barotropic structure throughout the tropo- and lower stratosphere. The second EOF (12%) is characterized by the North Atlantic Oscillation (NAO) and a polar dipole. These patterns are similar to the main spatial modes of the observational field of geopotential height at 500 hPa provided by Perlwitz (2000) and of the observed and simulated fields of sea level pressure determined in Fyfe *et al.* (1999), even though the variance explained by the first two EOFs is higher than in observations.

The most dominant spatial mode of the SCM simulation, explaining about 79% of total variance, shows low pressure systems over the Arctic continents. With the midlatitude centres over the Atlantic and Pacific shifted towards the eastern boundaries of the oceans, the first EOF bears some resemblance to the AO. The second EOF (7%) has a more zonally symmetric annular structure. The differences between the main spatial patterns of the SCM and the observations on the one hand and the large value of explained variance by EOF 1 on the other hand may give hints that the role of the planetary waves and its interaction with the zonal mean flow are underestimated by this model.

In order to define circulation regimes, the probability density function (PDF) based on the projection time series (principal components; PC) of the first two EOF has been calculated with a Gaussian kernel estimator (Silverman, 1986). For this kind of computation the choice of the smoothing parameter h is crucial. We used medium values of the smoothing parameters, i.e. $h = 0.30$ for a data length of 300 (100 years) and $h = 0.20$ for the 3000 data of the full 1000 years. The question if the phase space has a uni- or multimodal structure has been answered by means of a smoothed bootstrap test on multi-modality according to Silverman (1981). As a first step this test involves the determination of critical values of the smoothing parameter h_k from the data in the sense that h_k is the smallest value of h that gives k modes. For testing the null hypothesis “the distribution has k modes” against the alternative of “ $k + 1$ modes” one has to decide whether the value of h_k is significantly large in comparison with the corresponding values for random samples of the same distribution as the data. The significance level of h_k is estimated by the proportion of those bootstrap generated values that are $\geq h_k$. Silverman (1981) has shown that this is equal to the number of generated data sets for which the PDF calculated with a smoothing parameter of h_k has more than k modes. In the following all significance levels have been determined by using 1000 bootstrap samples.

As a test of departures of the full 1000-year-PDFs from Gaussianity we applied a probability plotting technique (quantile–quantile plot or qq-plot). That is the Mahalanobis distances of the model data are plotted against the quantiles of a χ^2 distribution with two degrees of freedom (e.g. Hartung and Elpelt, 1995). The null hypothesis is that the data are normally distributed, i.e. the Mahalanobis distances follow a χ^2 distribution. Deviations from a normal distribution results in departures from a 1:1 line. As a “theoretical bivariate sample” we used 1000 Monte Carlo simulations of normal distributed data with the same sample length as the model data. From these synthetic data the mean qq-slope and the 90% confidence levels of fluctuations around it have been determined.

For those cases where no significant multimodality could be detected, the question arises whether or not the phase space location of the centroids differs from purely Gaussian noise. The null hypothesis of a simple test implies that the phase space position of the unimodal maxima cannot be distinguished from the location due to a Gaussian noise process. A critical noise radius r_{crit} of the PDFs centroids has been calculated based on 1000 Monte Carlo simulations of normal distributions of the same length and smoothing parameters used. This radius gives a simple measure of the region in which the unimodal maximum of the PDF is to be expected with a certain level of confidence. The results of this test are very sensitive to the choice of the smoothing parameter h . For $h = 0.30$, i.e. 300 data points, the critical threshold radii are $r_{crit,90\%} = 0.64$ and $r_{crit,95\%} = 0.73$. If the maximum of the unimodal PDFs lies outside this given sphere, the distribution differs significantly from Gaussian noise.

4. DISCUSSION

Considering the total 1000-year-long integrations, we tested the PDFs on departures from Gaussianity using the qq-plot technique. Figure 1 shows the qq-plots for both models along with the mean value and 90% confidence level of a bivariate normal distributed sample. Taking into account that in principal graphical test methods are not as strict as analytical test methods, deviations from Gaussianity can be found for both models with a significance level of 10%, despite the fact that they are not considerably large. This finding is supported by significant deviations from univariate Gaussian distributions of the single projection coefficients using a Kolmogorov–Smirnov test modified after Lilliefors (1967).

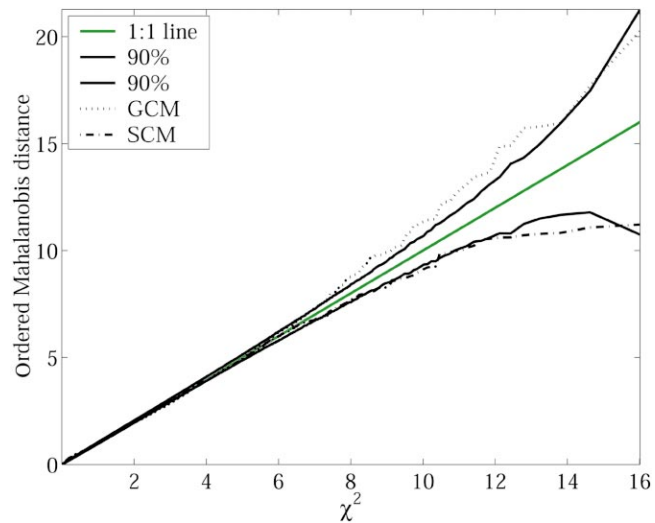


Figure 1. qq-plot for testing the 1000-year bivariate model data on Gaussianity. The plotted Mahalanobis distances have been calculated for 3000 monthly averaged winter PC data.

The PDFs show no multimodality for the GCM, but a bimodal structure for the SCM. For the latter the applied bootstrap test on bimodality yields that the null hypothesis of one mode can be rejected with a confidence of 95% and thus the alternative hypothesis of two or more modes can be accepted with a high level of confidence.

To investigate the temporal evolution and to make the length of the considered data more comparable to the length of the analysed observations, the time series of the PCs have been divided into 10 non-overlapping segments of each 100-year length. Although most of the segments display unimodal PDFs two segments with evidence on bimodality on the 5% bootstrap significance level could be detected for the GCM. In the case of the SCM the same test confirmed a bimodal structure for four of the ten segments on the 5% significance level and trimodality for one segment on the 10% significance level. In contrast to the observations, no segment with four distinct centroids has been found in either model. Figure 2 shows the two-dimensional PDF of the first 100-year segment as an example for bimodality in the GCM. The peaks in the PDF indicate the existence of at least two well-separated regimes. For further investigations only the most frequent modes have

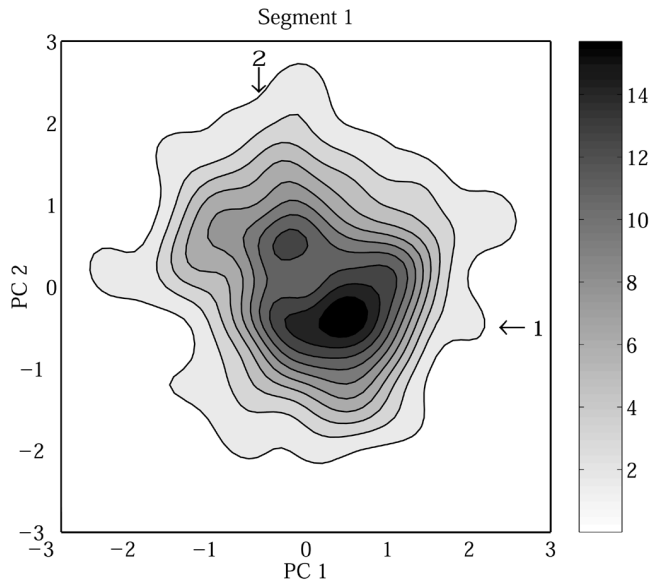


Figure 2. Probability density function (PDF) of the first 100-year segment of the ECHAM3/LSG simulation. The PDF has been calculated in the two-dimensional phase space spanned by detrended EOF 1 and EOF 2 for the whole 1000 years. PC 1 and PC 2 indicate the projection coefficients of 500-hPa geopotential height data onto EOF 1 and EOF 2, respectively.

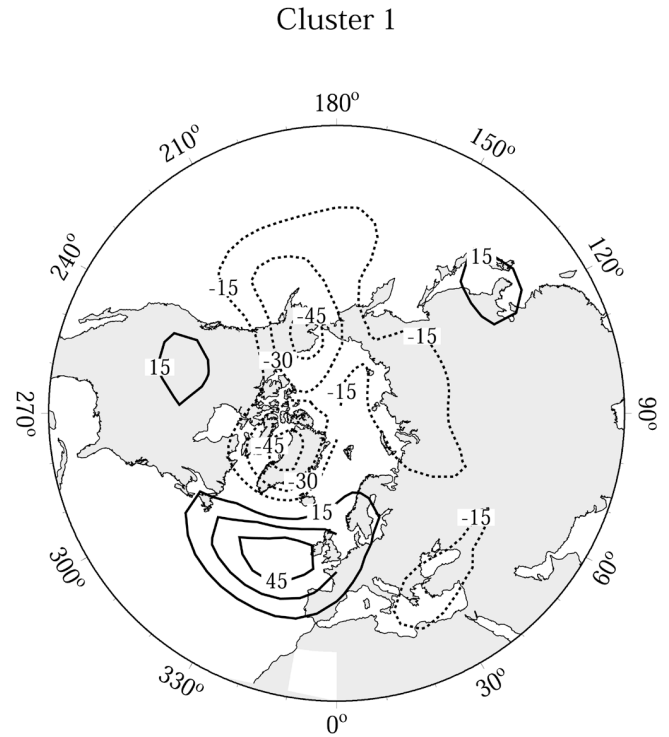


Figure 3. Mean pattern of 500-hPa geopotential height anomalies (in gpm) of those years belonging to cluster 1, indicated in [Figure 2](#).

been considered by defining threshold values relative to the absolute maximum of the PDF. Thus sufficiently large cluster sizes have been ensured. For the first segment of the GCM simulation this results in two distinct clusters, labelled in [Figure 2](#). The corresponding mean 500-hPa geopotential height anomaly fields bear resemblance to well-known teleconnection patterns. Cluster 1 ([Figure 3](#)) reminds one of the linear regression field between the 500-hPa height and the NH mean surface air temperature, known as the Cold Ocean Warm Land (COWL) pattern. The most striking features of cluster 2 ([Figure 4](#)) are the NAO in its negative phase and a polar dipole similar to EOF 2.

For the SCM, [Figure 5](#) displays the trimodal PDF in the tenth 100-year segment. Here, the second cluster anomaly field mainly projects onto EOF 1, whereas the two other composites primarily reproduce the EOF 2 in both phases. Thus, cluster 2 corresponds to negative 5.5-km pressure anomalies over most of the Arctic and Siberia and positive anomalies over the midlatitude eastern boundaries of the oceans.

A test has been performed for those segments which have unimodal distributions in order to decide whether or not the phase space locations of these centroids differ significantly from Gaussian noise. [Table 1](#) summarizes the calculated distances of the positions of the PDF maxima from the origin.

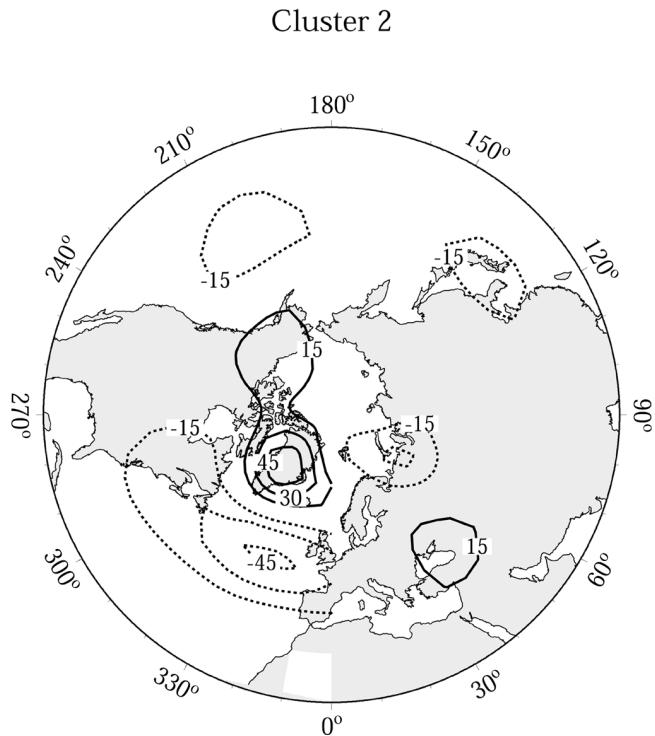


Figure 4. Mean pattern of 500-hPa geopotential height anomalies (in gpm) of those years belonging to cluster 2, indicated in Figure 2.

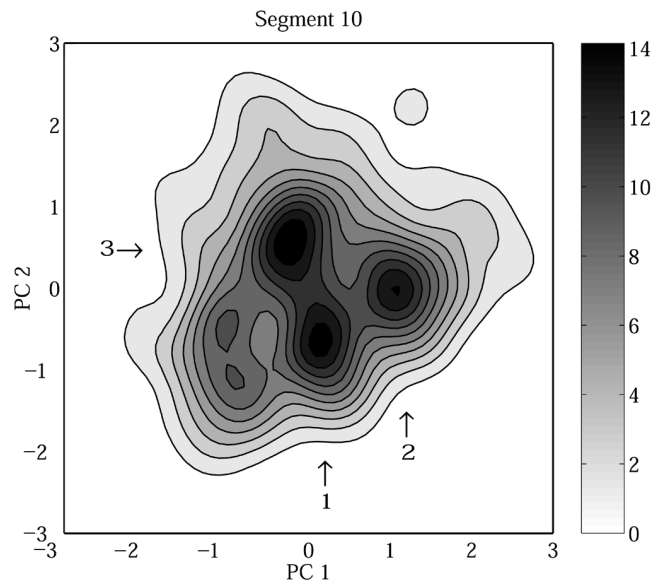


Figure 5. Probability density function (PDF) of the second 100-year segment of the SCM simulation. The PDF has been calculated in the two-dimensional phase space spanned by detrended EOF 1 and EOF 2 for the whole 1000 years. PC 1 and PC 2 indicate the projection coefficients of 5.5-km pressure data onto EOF 1 and EOF 2, respectively.

In the case of the SCM, for three of the five tested segments centroids out of the critical radius $r_{crit,90\%}$ have been detected. Among them two segments show the same anomaly patterns which project mainly on EOF 2 in its positive phase. The existence of coherent departures from Gaussianity is further confirmed by *multimodal* segments which show centroids out of the critical radius connected with the same pattern. In contrast, the GCM reveals only one of the eight tested segments to have a PDF maximum located outside the 90% confidence radius of a Gaussian centroid. The corresponding geopotential height anomaly indicates a westward shift of the NAO centres. The remaining seven PDF centroid locations in the phase space cannot be distinguished from purely noise.

5. SUMMARY AND CONCLUSIONS

Two long-term control integrations of climate models of different complexity have been analysed in respect of NH winter atmospheric circulation regimes. For both models indications of departures of the bivariate probability density functions in a reduced phase space from

Table 1. Distance from the two-dimensional PDF origin calculated for segments with unimodal distributions ($h = 0.30$)

Segment	SCM	GCM
1	0.65	—
2	0.65	—
3	—	0.59
4	0.60	0.88
5	—	0.34
6	0.80	0.25
7	—	0.43
8	0.51	0.32
9	—	0.56
10	—	0.43

a Gaussian distribution have been found. Considering the full 1000 years, the PDF of the SCM has a bimodal structure and the unimodal GCM distribution shows deviations from a bivariate normal distribution.

To explore the regime behaviour on decadal time scales in more detail, 10 sub-segments of 100-year length have been constructed and analysed. In the case of the SCM, the PDF undergoes strong temporal variations from segment to segment. In 50% of the cases bi- and trimodal distributions have been proved. The corresponding tropospheric pressure fields reflect mainly the patterns of EOF 1 and EOF 2, respectively. The GCM reveals considerably less variability. Two bimodal segments with significant deviations from unimodality have been detected. The corresponding composites resemble characteristic teleconnection patterns similar to COWL and NAO.

It has been shown that several unimodal coherent departures from Gaussianity on the 100-year time scale can be detected for the SCM. In contrast, the GCM generated only one 100-year segment for which the density distribution proves to be significantly different from random noise.

Both models do not reproduce the variety of observed anomaly patterns as shown in Corti *et al.* (1999). While the SCM reveals in particular large differences between observed and simulated large scale patterns, the GCM seems to be more stochastic in the sense that most of the variations cannot be distinguished from Gaussian noise processes. Spectral analyses of the ultra-low-frequency variations (Weisheimer, 2000) support this loss of statistical significant internal variability on time scales longer than a decade. However, the incidence of significant unimodal non-Gaussian distributions cannot be excluded entirely according to the analysis described.

Given that the analysis by Corti *et al.* (1999) based on NCEP reanalysis data was conducted over 45 years, the question may arise from the described investigations whether multimodality would be more pronounced if the subsamples covered a comparable period. Using twenty 50-year segments for extended winter data of the GCM affirms the robustness of the PDF structure. Only three of the twenty segments show statistical significant bimodal PDFs and 15 of the remaining unimodal subsamples cannot be distinguished from random noise.

Keeping in mind the shortness of available atmospheric data set as well as that the used data from 1949 to 1994 are not *a priori* free of any imposed forcing itself and thus comparisons to control model runs may be somewhat ambiguous, the issue whether the differences between the simulated and observed variability are due to deficiencies of the used models cannot be completely clarified in this study. Nevertheless,

in order to be able to answer the question as to how an imposed external forcing influences the regime behaviour, it is suggested to use climate models with improved representation of long-term variability processes.

Acknowledgements

We thank J. Perlwitz and R. Voss from the Max Planck Institute for Meteorology, Hamburg for providing the GCM data and appreciate the support of V. K. Petoukhov, I. I. Mokhov and A. V. Eliseev from the Institute of Atmospheric Physics, Moscow in performing long term runs of the SCM. The comments of the reviewer and Th. Kumke have been helpful and constructive. This work was partly sponsored by the strategy fund project “Natural climate variations from 10,000 years to the present day” of the Helmholtz Association of German Research Centres.

REFERENCES

- Corti, S., Molteni, F. and Palmer, T. N., 1999. Signature of recent climate change in frequencies of natural atmospheric circulation regimes. *Nature*, **398**, 799–802.
- Fyfe, J. C., Boar, G. J. and Flato, G. M., 1999. The arctic and Antarctic oscillations and their projected changes under global warming. *Geophys. Res. Lett.*, **26**, 1601–1604.
- Handorf, D., Petoukhov, V. K., Dethloff, K., Eliseev, A. V., Weisheimer, A. and Mokhov, I. I., 1999. Decadal climate variability in a coupled atmosphere-ocean climate model of moderate complexity. *J. Geophys. Res.*, **104**, 27253–27275.
- Hartung, J. and Elpelt, B., 1995. *Multivariate Statistik*. München Wien: Oldenbourg Verlag, 815 pp.
- Lilliefors, H. W., 1967. On the Kolmogorov-Smirnov test for normality with mean and variance unknown. *J. Amer. Statist. Assoc.*, **62**, 399–402.
- Lorenz, E. N., 1968. Climate determinism. *Meteorol. Monogr.*, **30**, 1–3.
- Maier-Reimer, E., Mikolajewicz, U. and Hasselmann, K., 1993. Mean circulation of the Hamburg LSG model and its sensitivity to the thermohaline surface forcing. *J. Phys. Oceanogr.*, **23**, 731–757.
- Monahan, A. H., Fyfe, J. C. and Flato, G. M., 2000. A regime view of Northern Hemisphere atmospheric variability and change under global warming. *Geophys. Res. Lett.*, **27**, 1139–1142.
- Palmer, T. N., 1999. A nonlinear dynamical perspective on climate prediction. *J. Climate*, **12**, 575–591.
- Perlwitz, J., 2000. The dynamical link between the troposphere and stratosphere and its potential to affect climate. *MPI-Examensarbeit 74*, Max-Planck-Institute for Meteorology, Hamburg, Germany, 145 pp.
- Perlwitz, J., Graf, H.-F. and Voss, R., 2000. The leading mode of the coupled troposphere-stratosphere winter circulation in different climate regimes. *J. Geophys. Res.*, **105**, 6915–6926.
- Petoukhov, V. K., Mokhov, I. I., Eliseev, A. V. and Semenov, V. A., 1998. The IAP RAS Global Climate Model. Techn. Rep. Moscow State Univ., Moscow, Russia, 110 pp.
- Roeckner, E., Arpe, K., Bengtsson, L., Brinkop, S., Dümenil, L., Esch, M., Kirk, E., Lunkeit, F., Ponater, M., Rockel, B., Sausen, R., Schlese, U., Schubert, S. and Windelband, M., 1992. Simulation of the present-day climate with the ECHAM model: Impact of model physics and resolution *MPI-Report*, **93**, Max-Planck-Institute for Meteorology, Hamburg, Germany, 171 pp.
- Silverman, B. W., 1981. Using kernel density estimates to investigate multimodality. *J. Roy. Statist. Soc.*, **43**, 97–99.
- Silverman, B. W., 1986. *Density Estimation for Statistics and Data Analysis*. New York, USA: Chapman & Hall, 175 pp.

- Thompson, D. W. J. and Wallace, J. M., 1998. The Arctic Oscillation signature in the winter-time geopotential height and temperature fields. *Geophys. Res. Lett.*, **5**, 1297–1300.
- Timmerman, A., Latif, M., Voss, R. and Grötzner, A., 1998. Northern hemispheric interdecadal variability: a coupled Air-Sea Mode. *J. Climate*, **11**, 1906–1931.
- Weisheimer, A., 2000. Ultra-low-frequency variability of large scale atmospheric circulation patterns in spectral low-order moels (in German). *Reports on Polar Research*, **356**, 174.